
Monograph:
Yue, R., Billings, S.A. and Zi, Qiang Lang (2004) An Investigation into the Characteristics of Nonlinear Frequency Response Functions, Part 1: Understanding the Higher Dimensional Frequency Spaces. Research Report. ACSE Research Report 854 . Department of Automatic Control and Systems Engineering

---

An Investigation into the Characteristics of Nonlinear Frequency Response Functions, Part 1: Understanding the Higher Dimensional Frequency Spaces

R.Yue, S.A.Billings and Zi-Qiang Lang

Department of Automatic Control and Systems Engineering
The University of Sheffield
Sheffield S1 3JD
U.K.

Research Report No.854
March 2004

An Investigation into the Characteristics of Nonlinear Frequency Response Functions, Part 1: Understanding the Higher Dimensional Frequency Spaces

R.Yue, S.A.Billings and Zi-Qiang Lang

Department of Automatic Control and Systems Engineering, The University of Sheffield, Sheffield S1 3JD,U.K.

Abstract

The characteristics of generalised frequency response functions (GFRFs) of nonlinear systems in higher dimensional space are investigated using a combination of graphical and symbolic decomposition techniques. It is shown how a systematic analysis can be achieved for a wide class of nonlinear systems in the frequency domain using the proposed methods. The paper is divided into two parts. In Part 1, the concepts of input and output frequency subdomains are introduced to give insight into the relationship between one dimensional and multi-dimensional frequency spaces. The visualisation of both magnitude and phase responses of third order generalised frequency response functions is presented for the first time. In Part 2 symbolic expansion techniques are introduced and new methods are developed to analyse the properties of generalised frequency response functions of nonlinear systems described by the NARMAX class of models. Case studies are included in Part 2 to illustrate the application of the new methods.

Keywords: Nonlinear Systems, Generalized Frequency Response Functions, Frequency Domain Analysis

1. Introduction

The study of nonlinear systems has received increasing attention since the early twentieth century, largely because traditional linear systems theory is unable to explain many important nonlinear phenomena such as harmonic distortion, limit cycle behaviour, and chaos.

Linear frequency response functions are recognised as one of the most powerful and successful tools to describe system behaviours by both analytical and graphical means. The introduction of the generalised frequency response functions in the late 1950s (George 1959) was the beginning of studies to extend frequency domain methods to nonlinear systems. The Generalised Frequency Response Functions (GFRFs) are defined as the multiple Fourier transforms of the kernels in the Volterra series and represent a natural generalisation of linear frequency response functions to the nonlinear case. The analysis of nonlinear systems in the frequency domain employing generalised frequency response functions dates back to the 1960s, when the Volterra functional series was originally applied to solve nonlinear problems encountered in communication systems and nonlinear circuits (Narayanan 1967, 1970, Bedrosian and Rice 1971). Much effort has subsequently been made to extend these methods to more general cases (Bussgang *et al*, 1974, Chuo and Ng 1979a,b). The significant results which have been achieved form the framework for the analysis of the steady-state output response for a class of weakly nonlinear circuits. Many studies have also been made to develop techniques for estimating the GFRFs of an unknown nonlinear system from input/output data (Brillinger 1970, Vinh *et al*1987, Kim and Powers 1988, Chuo and Liao

1989, Bendat 1990, and Nam and Powers 1994). Most of the methods are based on multidimensional FFT/windowing type algorithms and involve the computation of higher order spectra. These approaches can provide estimates of the GFRFs up to third order but work only on the assumption that the system under study can be described by a truncated Volterra series of low order and/or that special input excitation signals can be used. In addition to these restrictive assumptions, the considerable computational cost associated with these nonparametric methods makes it very difficult to extend the methods to more realistic higher order cases. An alternative technique is the parametric approach proposed by Billings and Tsang (1989a), which consists of estimating the parameters in a NARMAX model description of the system and then deriving the GFRFs from the estimated model directly using a probing method. This approach can produce the analytical expressions for GFRFs in terms of the coefficients of the system time domain model and avoids most of the complexity associated with previous methods. This approach provides a unified method of determining the GFRFs of any order for a wide class of nonlinear system.

Despite the significant results that have been obtained, it has not been shown how the GFRFs themselves can be effectively interpreted. The nature of the GFRFs and the connection of these to nonlinear behaviours are still not well understood. This is one possible reason why few applications can be found based on the GFRFs. There are two main difficulties. First, the GFRFs are actually a sequence of multivariable functions defined in high dimensional frequency space. Second, only expressions in the recursive form are available for the GFRFs and expansions of these expressions, which could reveal much more insight, have not been studied. Some authors have recently attempted to overcome some of these difficulties. Peyton Jones and Billings (1990) interpreted the n-dimensional frequency domain by defining subdomains, which relate directly to the system input/output behaviour. Zhang and Billings (1993) decomposed the second-order GFRFs into a set of typical components and explained the contribution by each of the components to the overall features of the GFRFs by graphical means. Although these studies lead to some constructive results, the structure of the GFRFs remained largely concealed and there has been no systematic way of investigating GFRF's of arbitrary order. Furthermore, since many nonlinear systems exhibit properties that require a Volterra series up to third order, which involves the lowest odd order nonlinear term in the Volterra series model, methods which allow the examination of the characteristics of third order GFRF's, are required.

The objectives of this paper are to explore the techniques which can reveal the inherent formation of the GFRFs, to investigate the visualisation of third order GFRF's, and to present a cohesive method for studying the family of GFRFs The paper is divided into two parts. Part 1 introduces the concepts of input/output subdomains. These concepts help gain an understanding of the multidimensional frequency domain and the connection to one-dimensional input/output spectra. Techniques for visually inspecting third order GFRF's in a 3D frequency space are presented for the first time in Part 1. The problems concerned with the frequency domain representation of a discrete-time nonlinear system are also discussed in the first part. Part 2 outlines a symbolic expansion technique to reveal the structures and properties of the GFRFs, where similarity can be found regardless of the order of the GFRF. The basic constituent elements of the GFRFs are then identified and categorised. Based on this consistency, a systematic method is described to analyse the characteristics of the GFRFs. The individual effect of terms from the nonlinear time domain model on the GFRFs is investigated. Case studies are used to illustrate the new methods.

2. Input/Output Representations of Nonlinear Systems in the Frequency Domain

2.1 Continuous-time Nonlinear Systems and the Associated Frequency Domain Representations

For nonlinear systems that can be represented by the Volterra series in the continuous-time domain, the output is given by (Schetzen 1980, Rugh 1981):

$$y(t)=\sum_{n=1}^{\infty}\int_{-\infty}^{\infty}\cdots\int h_n(\tau_1,\cdots,\tau_n)\prod_{i=1}^{n}u(t-\tau_i)d\tau_i \tag{2.1}$$

where $h_n(\tau_1,\tau_2,\cdots,\tau_n)$ is called the nth order Volterra kernel. Equation (2.1) can be expressed in the form of a sum of outputs from an infinite number of parallel subsystems, namely

$$y(t)=\sum_{n=1}^{\infty}y_n(t) \tag{2.2}$$

where the nth-order output $y_n(t)$ is a homogeneous functional of degree n, given by

$$y_n(t)=\int_{-\infty}^{\infty}\cdots\int h_n(\tau_1,\cdots,\tau_n)\prod_{i=1}^{n}u(t-\tau_i)d\tau_i \tag{2.3}$$

A system represented by (2.3) is called a degree-n homogeneous system. These 'nth-order outputs' take a similar form to the familiar convolution integral of a linear system. Therefore, the Volterra kernel $h_n(\tau_1,\tau_2,\cdots,\tau_n)$ is also called the nth order impulse response.

Just as in the linear case, the frequency domain representation of a degree-n homogeneous system can be obtained by means of the Fourier Transform; only this time the operation takes place in a multidimensional space. For the necessity of further derivation, an associated multidimensional time function is introduced to replace the left hand side of the equation (2.3)

$$y_n(t_1,\cdots,t_n)=\int_{-\infty}^{\infty}\cdots\int_{-\infty}^{\infty}h_n(\tau_1,\cdots,\tau_n)\prod_{i=1}^{n}u(t_i-\tau_i)d\tau_i \tag{2.4}$$

from which the real output $y_n(t)$ can be recovered from

$$y_n(t)=y_n(t_1,\cdots,t_n)\big|_{t_1=\ldots=t_n=t} \tag{2.5}$$

Applying the multidimensional Fourier Transform to both sides of equation (2.4) yields

$$Y_n(j\varpi_1,\cdots,j\varpi_n)=H_n(j\varpi_1,\cdots,j\varpi_n)\prod_{i=1}^{n}U(j\varpi_i) \tag{2.6}$$

where $H_n(j\varpi_1,\cdots,j\varpi_n)$ is called the nth order Generalised Frequency Response Function (GFRF) and is defined as the multidimensional Fourier Transform of the nth order Volterra kernel $h_n(\tau_1,\tau_2,\cdots,\tau_n)$

$$H_n(j\varpi_1,\cdots,j\varpi_n)=\int_{-\infty}^{\infty}\cdots\int_{-\infty}^{\infty}h_n(\tau_1,\cdots,\tau_n)e^{-j(\varpi_1\tau_1+\ldots+\varpi_n\tau_n)}d\tau_1\cdots d\tau_n \tag{2.7}$$

Conversely $y_n(t)$ can be obtained by means of an n-dimensional inverse Fourier Transform from equation (2.6)

$$y_n(t) = F^{-1}[Y_n(j\varpi_1,\cdots,j\varpi_n)]\big|_{t_1=\ldots=t_n=t} = \frac{1}{(2\pi)^n}\int_{-\infty}^{\infty}\cdots\int_{-\infty}^{\infty} Y_n(j\varpi_1,\cdots,j\varpi_n) \times e^{j(\varpi_1+\cdots+\varpi_n)t} d\varpi_1\cdots d\varpi_n \tag{2.8}$$

The time- and frequency-domain representations (2.4) and (2.6) provide two equivalent system descriptions, but the relationship between these by means of the Fourier transform is complicated in the sense of dimensionality. The frequency relationship (2.6) operates between two n-dimensional frequency variables $\prod_{i=1}^{n} U(j\varpi_i), Y_n(j\varpi_1,\cdots,j\varpi_n)$, while in the time domain the input and output $u(t), y(t)$ are one-dimensional. To convert between these requires not only a time/frequency transformation, but also a dimensional expansion/contraction. Making the change of variables

$$\varpi = \sum_{i=1}^{n}\varpi_i \tag{2.9}$$

with an inverse

$$\varpi_n = \varpi - \sum_{i=1}^{n-1}\varpi_i \tag{2.10}$$

gives, from equation (2.8)

$$y_n(t) = \frac{1}{(2\pi)^n}\int_{-\infty}^{\infty}\cdots\int_{-\infty}^{\infty} Y_n(j\varpi_1,\cdots,j\varpi_{n-1}, j[\varpi - \sum_{i=1}^{n-1}\varpi_i])\times e^{j\varpi t} d\varpi_1,\cdots d\varpi_{n-1}, d\varpi \tag{2.11}$$

Equation (2.11) can be re-written in the form of an inverse Fourier transform:

$$y_n(t) = \frac{1}{(2\pi)}\int_{-\infty}^{\infty} Y_n(j\varpi)e^{j\varpi t} d\varpi \tag{2.12}$$

where

$$Y_n(j\varpi) = \frac{1}{(2\pi)^{n-1}}\underbrace{\int_{-\infty}^{\infty}\cdots\int_{-\infty}^{\infty}}_{n-1} Y_n(j\varpi_1,\cdots,j\varpi_{n-1}, j[\varpi - \sum_{i=1}^{n-1}\varpi_i])d\varpi_1,\cdots,d\varpi_{n-1} \tag{2.13}$$

The right-hand side of (2.13) represents the integration of the function $Y_n(j\varpi_1,\cdots,j\varpi_{n-1}, j[\varpi - \sum_{i=1}^{n-1}\varpi_i])$ over a $(n-1)$-dimensional frequency space, which can be regarded as the projection of the hyperplane $\varpi = \varpi_1 + \cdots + \varpi_n$ onto the hyperplane $\varpi_n = 0$ in this space. It can be further shown that this integration is equal to the integration of $Y_n(j\varpi_1,\cdots,j\varpi_n)$ over the n-dimensional hyperplane $\varpi = \varpi_1 + \cdots + \varpi_n$ multiplied by a constant (Lang and Billings 1996), that is

$$Y_n(j\varpi) = \frac{1/n^{1/2}}{(2\pi)^{n-1}}\int_{\varpi_1+\cdots\varpi_n=\varpi} Y_n(j\varpi_1,\cdots,j\varpi_n)d\sigma_\varpi \tag{2.14}$$

where $d\sigma_\varpi$ denotes the area of a minute element on the n-dimensional hyperplane $\varpi = \varpi_1 + \cdots + \varpi_n$. Equation (2.14) provides a clear physical meaning in the way that

$Y_n(j\varpi)$ is generated by summing the $Y_n(j\varpi_1,\cdots,j\varpi_n)$ over the hyperplane $\varpi=\varpi_1+\cdots+\varpi_n$.

The standard Fourier Transform pair with a one dimensional system output can finally be given as

$$Y(j\varpi)=\sum_{n=1}^{\infty}Y_n(j\varpi) \tag{2.15}$$

$$y(t)=\frac{1}{2\pi}\int_{-\infty}^{\infty}Y(j\varpi)e^{j\varpi t}d\varpi \tag{2.16}$$

It should be noted that although the ϖ's on both sides of equation (2.15) have the same value domain, the ϖ in the right hand side varies with the order of $Y_n(j\varpi)$ under the restriction (2.9).

2.2 Discrete-time Nonlinear Systems and the Associated Frequency Domain Representations

Despite the fact that most physical systems evolve in continuous time, usually studies are carried out in the discrete-time domain so that the advantages of digital technologies can be used. As in the continuous-time case, it is possible to describe a discrete-time nonlinear system with memory by means of the discrete-time Volterra series expansion.

$$y(k)=\sum_{n=1}^{\infty}\sum_{i_1=0}^{\infty}\cdots\sum_{i_n=0}^{\infty}h_n(i_1,\cdots,i_n)\prod_{p=1}^{n}u(k-i_p) \tag{2.17}$$

where the output signal $y(k)$ and input signal $u(k)$ are real sequences, and $h_n(i_1,\cdots,i_n)$ is the nth-order Volterra kernel of the system. For simplicity, only casual systems and signals will be considered by setting the lower limits on the two inner summations in (2.17) to be zero instead of $-\infty$. Re-write equation (2.17) in the form,

$$y(k)=\sum_{n=1}^{\infty}y_n(k) \tag{2.18}$$

where the nth-order output $y_n(k)$ is given by

$$y_n(k)=\sum_{i_1=0}^{\infty}\cdots\sum_{i_n=0}^{\infty}h_n(i_1,\cdots,i_n)\prod_{p=1}^{n}u(k-i_p) \tag{2.19}$$

Notice that the convolution integral in (2.3) is now replaced by the convolution summation. The associated function in the form of a multi-dimensional discrete sequence is again used to expand the two sides of (2.19) to the multi-dimensional discrete-time domain.

$$y_n(k_1,\cdots,k_n)=\sum_{i_1=0}^{\infty}\cdots\sum_{i_n=0}^{\infty}h_n(i_1,\cdots,i_n)\prod_{p=1}^{n}u(k_p-i_p) \tag{2.20}$$

Apply the multidimensional DTFT to both sides of (2.20) to give

$$Y_n(j\varpi_1,\cdots,j\varpi_n)=H_n(j\varpi_1,\cdots,j\varpi_n)\prod_{i=1}^{n}U(j\varpi_i) \tag{2.21}$$

where the generalised frequency response function $H_n(j\varpi_1,\cdots,j\varpi_n)$, this time, is defined in the multidimensional digital frequency domain as the Discrete Time Fourier Transform of the discrete-time nth-order Volterra kernel $h_n(k_1,\cdots,k_n)$:

$$H_n(j\varpi_1,\cdots,j\varpi_n)=\sum_{k_1=0}^{\infty}\cdots\sum_{k_n=0}^{\infty}h_n(k_1,\cdots k_n)e^{-j(\varpi_1k_1+\cdots+\varpi_nk_n)} \tag{2.22}$$

Then, according to (2.5), the output $y_n(k)$ can be recovered as

$$\begin{aligned} y_n(k) &= IDTFT[Y_n(j\varpi_1,\cdots,j\varpi_n)]\big|_{k_1=\ldots=k_n=k} \\ &= \frac{1}{(2\pi)^n}\int_{-\pi}^{\pi}\cdots\int_{-\pi}^{\pi}Y_n(j\varpi_1,\cdots,j\varpi_n)e^{j(\varpi_1+\cdots+\varpi_n)k}d\varpi_1\cdots d\varpi_n \end{aligned} \tag{2.23}$$

It follows that by changing the variables, a link is built up between one-dimensional and multi-dimensional digital frequency spaces.

$$y_n(k)=\frac{1}{(2\pi)}\int_{-\pi}^{\pi}Y_n(j\varpi)e^{jk\varpi}d\varpi \tag{2.24}$$

$$Y_n(j\varpi)=\frac{1/n^{1/2}}{(2\pi)^{n-1}}\int_{\substack{\varpi_1+\cdots\varpi_n=\varpi\\ |\varpi|<\pi}}Y_n(j\varpi_1,\cdots,j\varpi_n)d\sigma_{\varpi} \tag{2.25}$$

Compared with (2.14), a restriction, $|\varpi|<\pi$, is added to the range of the hyperplanes over which the integration in (2.25) is performed, suggesting equation (2.25) is defined in the digital frequency space. More discussion will be given in detail on the features of higher dimensional digital frequency space later in §4.3.

Equation (2.21) and (2.23) clearly show how the input is related to the output by the nth-order GFRF. The GFRFs therefore serve as a powerful tool to describe nonlinear system input/output behaviours in the frequency domain.

The GFRFs $H_n(j\varpi_1,\cdots,j\varpi_n)$ may differ by the permutations of their arguments, but they are equivalent in representing the system because in each case the output $y_n(t)$ in equation (2.8) or $y_n(k)$ in (2.23) would be identical. It is however convenient to work with symmetric transforms where the order of the arguments in $H_n(j\varpi_1,\cdots,j\varpi_n)$ can be arbitrarily interchanged. It has become a common practice therefore to symmetrise the functions by adding all the asymmetric GFRFs over all permutations of the arguments and dividing by the number (Schetzen 1980) to give

$$H_n^{sym}(j\varpi_1,\cdots,j\varpi_n)=\frac{1}{n!}\sum_{\substack{all\ permutations\\ of\ \varpi_1\cdots\varpi_n}}H_n(j\varpi_1,\cdots,j\varpi_n) \tag{2.26}$$

It is also apparent from equation (2.7) and (2.22) that the properties of conjugate symmetry hold for GFRFs

$$H_n(-j\varpi_1,\cdots,-j\varpi_n)=H_n^*(j\varpi_1,\cdots,j\varpi_n) \tag{2.27}$$

where the asterisk denotes complex conjugation. This property allows us to consider only the non-negative frequency region when investigating the GFRFs.

3. Properties of the Nonlinear Frequency Response and Analysis of this using GFRFs

For the case of linear systems any input frequencies pass independently through the system thus no new frequencies are produced and there is no influence or interaction between the

input frequency components. However in the response of nonlinear systems some new frequencies such as harmonics and intermodulation frequencies may appear together with effects such as gain compression/expansion and desensitisation. These phenomena characterise the nonlinear frequency response and will be investigated using the GFRF's in this section.

3.1 Nonlinear Frequency Response Analysis

Consider an input composed of K different sinusoids

$$\begin{aligned} u(t) &= \sum_{i=1}^{K} |A_i| \cos(\varpi_i t + \angle A_i) \\ &= \sum_{i=1}^{K} \frac{1}{2}(A_i e^{j\varpi_i t} + A_i^* e^{-j\varpi_i t}) \\ &= \sum_{\substack{i=-K \\ i\neq 0}}^{K} \frac{A_i}{2} e^{j\varpi_i t} \end{aligned} \tag{3.1}$$

where $|A_i|$ is the amplitude, $\angle A_i$ is the phase, A_i^* is the complex conjugate of A_i, $\{-\varpi_K, \cdots, -\varpi_1, \varpi_1, \cdots, \varpi_K\}$ are the input frequencies, $A_{-i} = A_i^*$ and $\varpi_{-i} = -\varpi_i$. The concept of the frequency mix vector will be used in this analysis. The mix vector has been used by several authors (Bussgang et al 1974, Chua and Ng 1979, Wiener and Spina 1980) for the steady state analysis of a Volterra system with multi-tone inputs. It will also be assumed that the subset $\{\varpi_1, \varpi_2, \cdots, \varpi_K\}$ of input frequencies forms a frequency base. This means there is no set of rational numbers $\{r_1, \cdots, r_K\}$ (not all zero) such that

$$r_1\varpi_1 + r_2\varpi_2 + \cdots + r_K\varpi_K = 0 \tag{3.2}$$

The nth order module or frequency mix vector of the input frequencies is $M = (m_{-k}, \cdots, m_{-1}, m_1, \cdots, m_k)$, m_i are non-negative integers $m_i \geq 0$, $\sum_{\substack{i=-K \\ i\neq 0}}^{K} m_i = n$,

$$\varpi_M = \sum_{\substack{i=-K \\ i\neq 0}}^{K} m_i\varpi_i = \sum_{i=1}^{K} (m_i - m_{-i})\varpi_i \tag{3.3}$$

and the sum of all terms with frequency ϖ_M for the nth output component $y_n(t)$ is given by

$$y_n(t;\varpi_M) = \frac{n!}{2^n}\left[\sum_{\substack{i=-K \\ i\neq 0}}^{K} \frac{A_i^{m_i}}{m_i!}\right] H_n(m_{-k}\{\varpi_{-k}\}, \cdots, m_{-1}\{\varpi_{-1}\}, m_1\{\varpi_1\}, \cdots, m_k\{\varpi_k\}) e^{j\varpi_M t} \tag{3.4}$$

where $m_j\{\varpi_j\}$ denotes m_j consecutive arguments with the same frequency ϖ_j.

The nth order components of the output response $y_n(t)$ consists of all possible frequency mixes and is given by

$$y_n(t)=\sum_{m_{-K}=0}^{n}\cdots\sum_{m_{-1}=0}^{n}\sum_{m_1=0}^{n}\cdots\sum_{m_K=0}^{n}y_n(t;\varpi_M) \tag{3.5}$$

where only terms for which the indices sum to n are included in the summation. The total output response at frequency $\varpi_M=\varpi_j$ is from equation (2.2),

$$y(t;\varpi_j)=\sum_{n=1}^{\infty}\sum_{\substack{All\ possible\ M\\ such\ that\varpi_M=\varpi_j}}y_n(t;\varpi_M) \tag{3.6}$$

Equation (3.6) illustrates that when a sum of K sinusoids is applied to a nonlinear system additional output frequencies are generated by the nth order GFRF $H_n(j\varpi_1,\cdots,j\varpi_n)$ of the system consisting of all possible combinations of the input frequencies $\{-\varpi_K,\cdots,-\varpi_1,\varpi_1\cdots\varpi_K\}$ taken n at a time. The new frequency ϖ_M will arise in the output spectra provided the frequency response function H_n has a value at the corresponding point $\{m_{-k}\{\varpi_{-k}\},\cdots,m_{-1}\{\varpi_{-1}\},m_1\{\varpi_1\},\cdots,m_k\{\varpi_k\}\}$ in the n-dimension domain.

Consider the input with only two-tone to simplify the analysis,

$$u(t)=|A_1|\cos(\varpi_1 t+\angle A_1)+|A_2|\cos(\varpi_2 t+\angle A_2) \tag{3.7}$$

The input frequencies to the system will then be $-\varpi_2,-\varpi_1,\varpi_1,\varpi_2$ as suggested by equation (3.1). As a result, the nth-order module vector of the input frequencies will take the form $M=(m_{-2},m_{-1},m_1,m_2)$ and the components of M satisfy,

$$m_{-2}+m_{-1}+m_1+m_2=n \tag{3.8}$$

The output $y_n(t;\varpi_M)$ becomes

$$y_n(t;\varpi_M)=\frac{n!}{2^n}\frac{A_{-2}^{m_{-2}}A_{-1}^{m_{-1}}A_1^{m_1}A_2^{m_2}}{m_{-2}!m_{-1}!m_1!m_2!}H_n(m_{-2}\{\varpi_{-2}\},m_{-1}\{\varpi_{-1}\},m_1\{\varpi_1\},m_2\{\varpi_2\})\times e^{j[(m_1-m_{-1})\varpi_1+(m_2-m_{-2})\varpi_2]t} \tag{3.9}$$

Based on the above equation, the aforementioned nonlinear phenomena will be interpreted below.

3.2 Harmonics

Harmonics are frequency components that are equal to multiples of the fundamental input frequency. If the mix vector is chosen as $M=(0,\frac{n-p}{2},\frac{n+p}{2},0)$, the pth harmonic of ϖ_1 ($p\varpi_1$) will be generated in the nth-order output response,

$$y_n(t;p\varpi_1)=\frac{n!}{2^n}\frac{A_{-1}^{\frac{n-p}{2}}A_1^{\frac{n+p}{2}}}{(\frac{n-p}{2})!(\frac{n+p}{2})!}H_n((\frac{n-p}{2})\{\varpi_{-1}\},\frac{n+p}{2}\{\varpi_1\})\times e^{jp\varpi_1 t} \tag{3.10}$$

Likewise, the pth harmonic of $\varpi_2 (p\varpi_2)$ will appear in the output if M takes the form $(\frac{n-p}{2},0,0,\frac{n+p}{2})$. Since m_i is constrained to be a non-negative integer, n must be greater than or equal to p and since m_i and m_{-i} are integers, n must be odd when p is odd and even when p is even. Odd harmonics must therefore be created by all odd order GFRFs and even harmonics must be created by all even order GFRFs.

3.3 Desensitisation

In linear systems the sinusoidal response at a particular frequency is unaffected by the application of sinusoidal signals at other frequencies. When a system is nonlinear however, the sinusoidal response at frequency ϖ_1 can be modified by the application of a second sinusoidal signal at frequency ϖ_2. This interference type phenomenon is referred to as desensitisation.

The nth-order output of a Volterra system with the two-tone input (3.7) is given by equation (3.9). It follows from equation (3.9) that the total response at frequency ϖ_1 includes contributions from all odd-order terms such as $H_1(\varpi_1)$, $H_3(-\varpi_1,\varpi_1,\varpi_1)$, $H_3(-\varpi_2,\varpi_1,\varpi_2),\cdots$. The first and third order contributions to the output response result from frequency mixes M=(0,0,1,0), (0,1,2,0) and (1,0,1,1).

Notice that the output of a real system is real for real inputs. Hence $y_n(t)$, the nth-order output of a Volterra nonlinear system, should be real and the complex terms in equation (3.9) must appear in conjugate pairs. The sinusoidal response at frequency ϖ_M can thus be obtained by combining equation (3.9) with its complex conjugate to give

$$\hat{y}_n(t;\varpi_M) = y_n(t;\varpi_M) + y_n(t;-\varpi_M) = y_n(t;\varpi_M) + y_n^*(t;\varpi_M) = 2\,\mathrm{Re}\{y_n(t;\varpi_M)\} \tag{3.11}$$

where $\hat{y}_n(t;\varpi_M)$ denotes the nth order sinusoidal response at frequency ϖ_M.

The total response at frequency ϖ_1, including only terms up to third order, can therefore be expressed as

$$\begin{aligned} y(t;\varpi_1) &= 2\,\mathrm{Re}\{y_1(t;\varpi_1) + y_3(t;(-\varpi_1+2\varpi_1)) + y_3(t;(-\varpi_2+\varpi_1+\varpi_2)) + \cdots\} \\ &= \mathrm{Re}\left\{\left[A_1 H_1(\varpi_1) + \frac{3}{4}A_1|A_1|^2 H_3(-\varpi_1,\varpi_1,\varpi_1) + \frac{3}{2}A_1|A_2|^2 H_3(-\varpi_2,\varpi_1,\varpi_2) + \cdots\right] e^{j\varpi_1 t}\right\} \end{aligned} \tag{3.12}$$

The last term in equation (3.12) is the third order desensitisation term. If $|A_1| << |A_2|$ such that the second term in equation (3.12) becomes negligible with respect to the desensitisation term, the sinusoidal response at frequency ϖ_1 assuming effects above third order can be neglected, then reduces to

$$y(t;\varpi_1) \approx \mathrm{Re}\left\{\left[A_1 H_1(\varpi_1) + \frac{3}{2}A_1|A_2|^2 H_3(-\varpi_2,\varpi_1,\varpi_2)\right] e^{j\varpi_1 t}\right\} \tag{3.13}$$

The gain of the system at frequency ϖ_1 is given as

$$S_{gain} = \frac{|y(t;\varpi_1)|}{|A_1|} = |H_1(\varpi_1)|\left|1 + \frac{3}{2}|A_2|^2 \frac{H_3(-\varpi_2,\varpi_1,\varpi_2)}{H_1(\varpi_1)}\right| \tag{3.14}$$

The above equation shows that the system gain at frequency ϖ_1 depends nonlinearly on the magnitude of the interfering signal at frequency ϖ_2 due to the GFRF $H_3(-\varpi_2,\varpi_1,\varpi_2)$.

3.4 Gain Compression/Expansion

Gain compression and expansion are terms used to describe the variation in the gain of a system as the input amplitude is increased. The system gain at the fundamental frequency varies as a function of the input amplitude in a nonlinear system, instead of increasing in a linear way as would be the case in a linear system. The effect where the system gain falls below that of the linear system is referred to as gain compression and an increase in gain due to the nonlinear behaviour of the system is called gain expansion. To illustrate these phenomena, apply the single sinusoidal input given by

$$u(t) = |A|\cos(\varpi t + \angle A) \tag{3.15}$$

The response of interest is the fundamental response which, from (3.4) and (3.11), is expressed as

$$y(t;\varpi) = \mathrm{Re}\left\{ A\left[H_1(\varpi) + \frac{3}{4}|A|^2 H_3(-\varpi,\varpi,\varpi) + \frac{5}{8}|A|^4 H_5(-\varpi,-\varpi,\varpi,\varpi,\varpi) + \cdots \right] e^{j\varpi t} \right\} \tag{3.16}$$

The gain of the system at the fundamental frequency ϖ is

$$S^{\varpi}_{gain} = \left| \frac{y(t,\varpi)}{A} \right| = \left| H_1(\varpi) + \frac{3}{4}|A|^2 H_3(-\varpi,\varpi,\varpi) + \frac{5}{8}|A|^4 H_5(-\varpi,-\varpi,\varpi,\varpi,\varpi) + \cdots \right| \tag{3.17}$$

For a linear system all generalized frequency response functions above order one will be equal to zero and the gain S^{ϖ}_{gain} at the fundamental frequency ϖ will be a constant that is equal to the magnitude of the linear frequency response function evaluated at frequency ϖ. The output amplitude will then be linearly proportional to the input amplitude $|A|$. However, the GFRFs will be non-zero for a nonlinear system and so the gain at the fundamental frequency ϖ will depend nonlinearly on the magnitude of the input signal.

3.5 Intermodulation

The process by which two or more signals combine in a nonlinear manner to produce new frequency components is termed as intermodulation.

It is obvious that the system *n*th-order output (3.9) under the excitation of two-tone input (3.7) includes new frequency components at the intermodulation frequency

$$\varpi_M = (m_1 - m_{-1})\varpi_1 + (m_2 - m_{-2})\varpi_2 \tag{3.18}$$

Having already introduced the phenomena of harmonics, gain compression /expansion and desensitisation, a more restrictive interpretation for intermodulation will be given here. Specifically intermodulation is used to refer to only those nonlinear frequency components, resulting from frequency mixes, that are not included in the above categories. For example components produced by the frequency mixes $(\varpi_1+\varpi_1+\varpi_1),(\varpi_1+\varpi_1-\varpi_1),(\varpi_2+\varpi_1-\varpi_2)$ *and* $(\varpi_2+\varpi_2-\varpi_1)$ are classified as belonging to the categories of harmonic, gain compression/expansion, desensitisation and intermodulation respectively.

4. Multi-dimensional Frequency Domain Space and Visual Representation

Both the input and output spectra of any nonlinear system are one-dimensional and have clear physical meaning. However, the multi-dimensional nature of the GFRFs and the system input/output frequency domain description shown in equations (2.7) and (2.8) raise questions relating to the mechanism by which the one-dimensional output spectra is produced from interactions of the system GFRF with input spectra in a high-dimensional frequency space. In this section, a theoretical foundation built upon previous work will be presented to provide insights into the mechanisms associated with the multi-dimensional frequency domain. Two important conceptions—input/output frequency subdomains are described initially and then, as supplements to the theory, special consideration for discrete-time nonlinear systems are discussed. Finally, graphical techniques to display the third order GFRF are introduced.

4.1 Input Frequency Subdomains

Input frequency subdomains in an n-dimensional frequency space over which the relationship (2.6) is established, are defined as domains where the input spectra $U(j\varpi_i), i=1,2,...,n$ in equation (2.6) exists and can be described by

$$\begin{cases} \varpi_a \le \varpi_i \le \varpi_b \\ \quad and \qquad i=1,2,...,n \\ -\varpi_b \le \varpi_i \le -\varpi_a \end{cases} \tag{4.1}$$

if the input of a nonlinear system has the continuous spectrum in $[\varpi_a, \varpi_b]$, or

$$\varpi_i \in \{\pm\varpi_{j1}, \pm\varpi_{j2}, ..., \pm\varpi_{jm}\},\ i=1,2,...,n \tag{4.2}$$

if the input is a multi-tone sinusoidal signal with a discrete spectrum at $\{\pm\varpi_{j1}, \pm\varpi_{j2}, ..., \pm\varpi_{jm}\}$. Obviously the total number of input frequency subdomains in an n-dimensional frequency space is n, as each of the input spectra $U(j\varpi_i), i=1,2,...,n$ has its own input frequency subdomain along the ϖ_i-axis. If the input signal is a white noise, the input frequency subdomains will be the whole n-dimensional frequency space. In this sense, an n-dimensional frequency space over which equation (2.6) is defined can be called an input frequency domain. Fig. 1(a) illustrates this concept for the case of a two-dimensional frequency space with a general band-limited input whose spectrum lies in the frequency interval $[\varpi_a, \varpi_b]$ and $[-\varpi_b, -\varpi_a]$. A much simpler example is shown in Fig. 1(b), where the system is excited by a two-tone input with discrete spectra at $\pm\varpi_b$ and $\pm\varpi_a$.

It is observed that the system is only excited at the common areas or the intersection points of the input frequency subdomains corresponding to the Cartesian product $\prod_{i=1}^{n} U(j\varpi_i)$ in (2.6). It is also in these areas that the nonlinear phenomena described in the previous section occur.

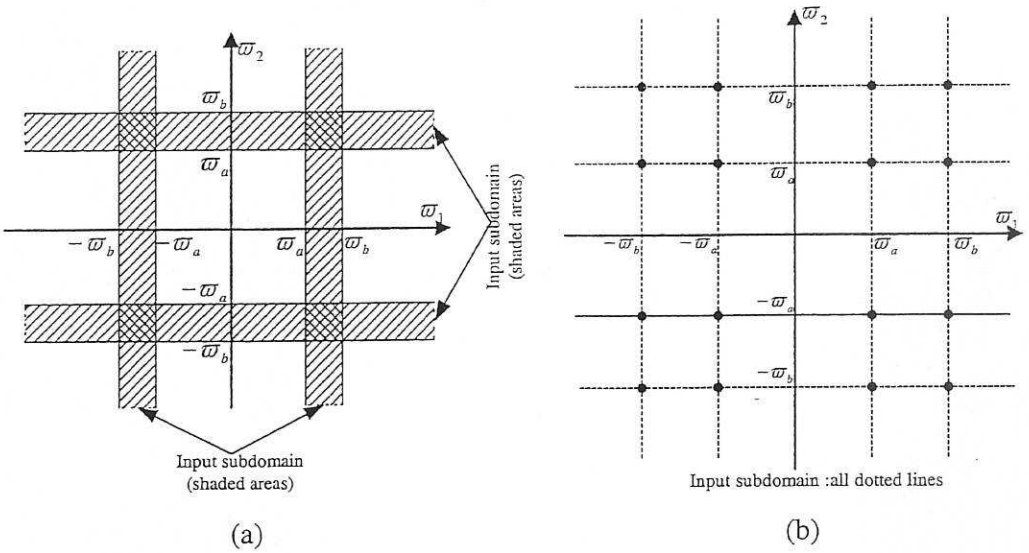

Fig. 1 Input frequency subdomains in a two-dimensional frequency space
(a) a general band-limited input. (b) a two-tone input

4.2 Output Frequency Subdomains

Recall that from equation (2.14) the system nth order output spectrum $Y_n(j\varpi)$ at the frequency component ϖ_{out} can be determined by the integration of the multivariable function $Y_n(j\varpi_1,\cdots,j\varpi_n)$ over the hyperplane in an n-dimensional frequency space. This is given by

$$\varpi_{out}=\varpi_1+\cdots+\varpi_n=\sum_{i=1}^{n}\varpi_i \tag{4.3}$$

and any set of points of $Y_n(j\varpi_1,\cdots,j\varpi_n)$ whose coordinates conform to (4.3) contribute to the same output frequency ϖ_{out}. The hyperplane (4.3) will therefore be called an output frequency subdomain.

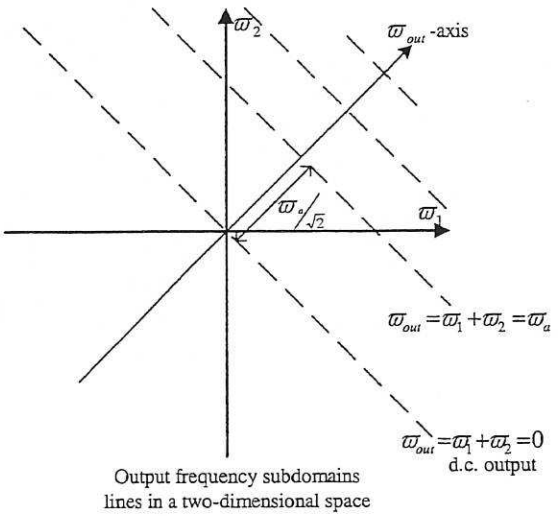

Fig. 2 Output frequency subdomains in a two-dimensional space

Fig. 2 illustrates the concept of output frequency subdomain for the case of a second order system, where the output frequency subdomains are given by lines $\varpi_{out} = \varpi_1 + \varpi_2$

The distance from the origin to an output frequency subdomain, the dashed lines in Fig. 2, can be decided by geometrical means to be $\varpi_{out}/\sqrt{2}$. As a consequence, the line $\varpi_1 = \varpi_2$, which is orthogonal to all output frequency subdomains, can be perceived as the ϖ_{out}-axis, on which the coordinate proportionally indicates the real output frequency ϖ_{out} by a constant $1/\sqrt{2}$.

A more complicated example for a three-dimensional frequency space is shown in Fig. 3, where the output frequency subdomains become planes described by $\varpi_{out} = \varpi_1 + \varpi_2 + \varpi_3$ while the ϖ_{out}-axis this time runs along the line $\varpi_1 = \varpi_2 = \varpi_3$. It is also worth mentioning that the distance from the output frequency subdomain to the origin now becomes $\varpi_{out}/\sqrt{3}$.

In general, although the dimensions of the output frequency subdomains increase with the order of the output (from a line to a plane or even a hyperplane), the ϖ_{out}-axis will always be the line orthogonal to all output frequency subdomains, described by

$$\varpi_1 = \cdots = \varpi_n \tag{4.4}$$

and the distance from the origin to an output frequency subdomain (4.3) is given by $\varpi_{out}/\sqrt{n}$.

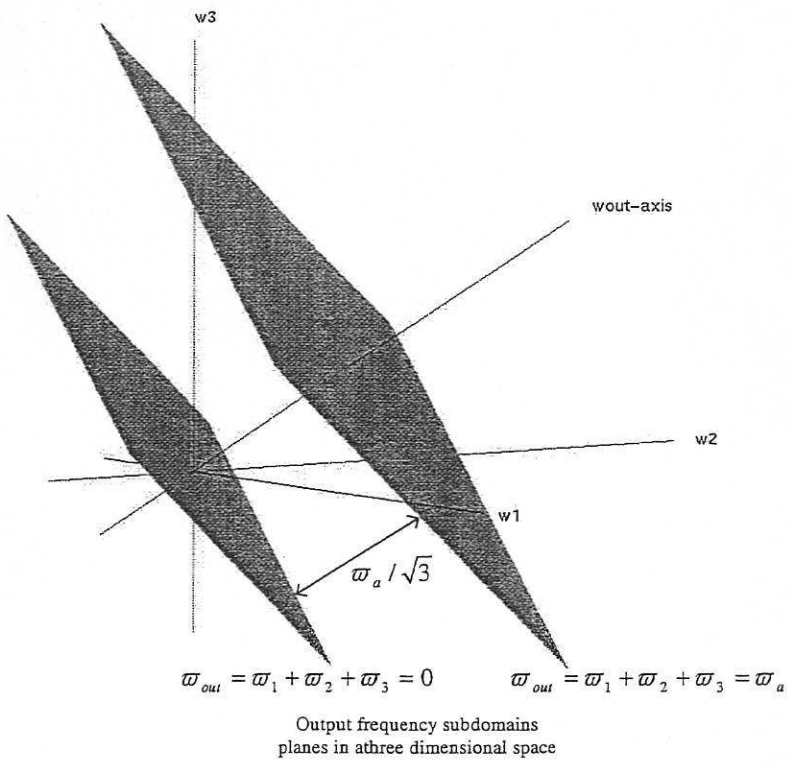

Fig. 3 Output frequency subdomains in a three-dimensional frequency space

Now that the concepts of input and output frequency domains have been introduced, some useful results can be instantly achieved based on this framework. Notice that the integrand $Y_n(j\varpi_1,\cdots,j\varpi_n)$ in (2.14), which is given by (2.6), is defined only at the intersection points of the input frequency subdomains in an n-dimensional frequency space (the cross squares in Fig. 1(a)). Therefore the integration in (2.14) will be restricted on the output frequency subdomains, which pass through the intersection of input frequency subdomains. That means the output frequency components, which a nonlinear system could generate, are decided uniquely by the system input spectrum, To illustrate this result, suppose that a second order system is excited by a two-tone input described by (3.7). The input and output frequency subdomains in this case are plotted in Fig. 4. Clearly, only those components, whose corresponding output frequency subdomains (dashed lines) pass through the intersection of the input subdomains (big dots), will appear in the system output. More significantly, some nonlinear phenomena, for example, harmonics (e.g., $2\varpi_a$, $2\varpi_b$) and intermodulations (e.g., $\varpi_a+\varpi_b$, $\varpi_b-\varpi_a$) are revealed in Fig. 4 to show that a considerable insight into the properties of the frequency response of a nonlinear system can be obtained using this new analysis method.

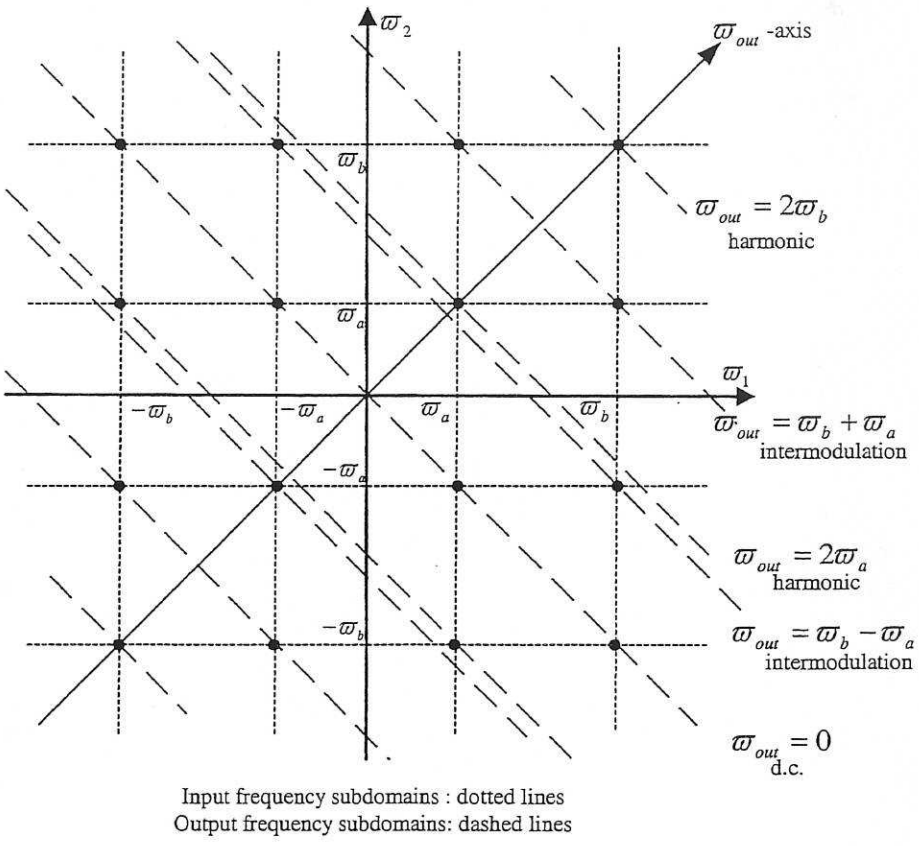

Fig. 4 Output frequency components of a second order system with a two-tone input

4.3 Associated Problems for The Discrete-time Nonlinear Models

The input/output frequency subdomains have been illustrated within the analogue frequency space corresponding to continuous-time systems. These ideas can be readily

extended to the digital frequency space. The multidimensional digital frequency space however has its own characteristics and care needs to be exercised when focusing on a discrete-time nonlinear system.

Consider again a second order Volterra system with an input signal, which has been lowpass-filtered to attenuate all frequency components above ϖ_{in_max}. The input and output frequency subdomains in a two-dimensional analogue frequency space are plotted in Fig. 5.

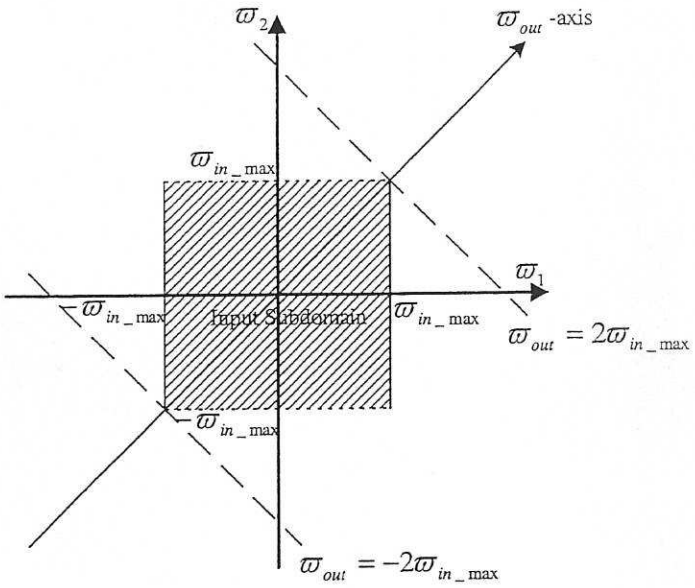

Fig. 5 The input and output subdomains of a second order Volterra system with input frequency components confined in $[0, \varpi_{in\_max}]$

From the analysis in §4.2, since the input signal has no frequency components above ϖ_{in_max}, the maximum frequency ϖ_{out_max} of the output for this second order Volterra system case satisfies the following relation,

$$\varpi_{out\_max} = 2\varpi_{in\_max} \tag{4.5}$$

as illustrated in Fig. 5. Therefore, if the input/output signals are uniformly sampled at the same sampling frequency ϖ_s, ϖ_s must meet the following requirement to avoid aliasing of the output signal

$$\varpi_s \geq 2\varpi_{out\_max} = 4\varpi_{in\_max} \tag{4.6}$$

Consider a discrete-time quadratic model derived by sampling the corresponding continuous-time second order Volterra system under the sampling condition (4.6), then the input/output frequency subdomains in a two-dimension digital frequency space will be as shown in Fig. 6(a)

According to digital signal processing theory, the sampling frequency is mapped to the digital frequency 2π and the DTFT of a discrete-time sequence or a sampled time signal is a periodic function of the digital frequency ϖ_d with period 2π. For a discrete-time quadratic Volterra system under the sampling condition (4.6), the input spectrum repeats itself with period 2π along each input frequency axis ϖ_i in a two-dimensional digital frequency space whereas the output spectrum is a periodic function of ϖ_{out} with period 2π.

Normalised frequency coordinates will be used in graphical representations of multidimensional frequency functions in this paper where the main interest is the relationship between the input and output frequency. This paper employs the convention that for discrete systems the unit frequency is the Nyquist frequency, namely the sampling frequency. All frequency quantities are normalized by the Nyquist frequency. For a system with a 1000 Hz sampling frequency, for example, 300 Hz would be represented as 300/1000 = 0.3. Normalized frequency is converted to digital angular frequency around the unit circle by multiplying by π. To convert normalized frequency back to Hertz, multiply by the sampling frequency, in this case 1000 Hz. Fig. 6(b) is simply a copy of Fig. 6(a) but with the units changed to be normalised frequency.

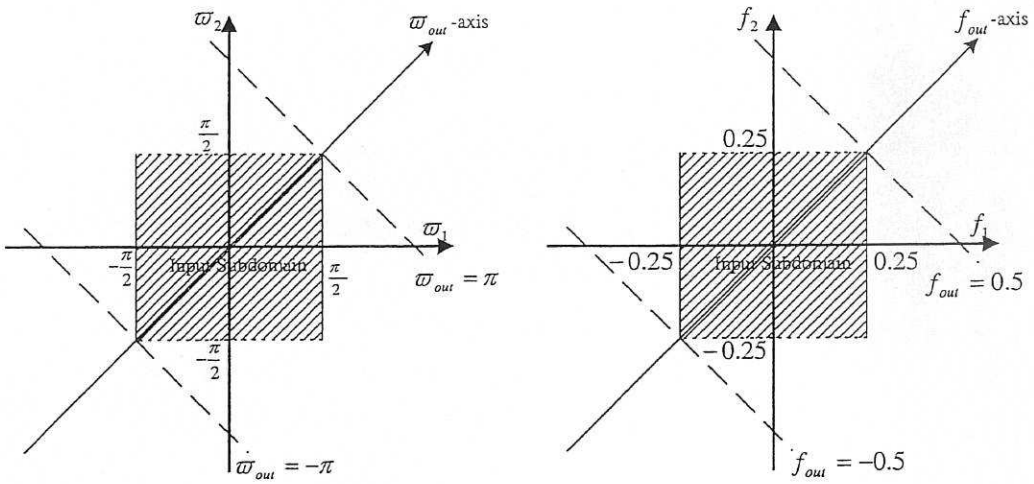

(a) unit in digital frequency (rad/s)

(b) normalised frequency

Fig. 6 The input/output subdomains of a quadratic discrete-time Volterra system in a two-dimensional digital frequency space.

More generally, for an *n*th-order Volterra system where only the input spectra are known beforehand, the following sampling condition must be satisfied in order to avoid aliasing at the output

$$\varpi_s \geq 2n \times \varpi_{in\_\max} \tag{4.7}$$

where $\varpi_{in\_\max}$ is the maximum frequency of the input signal. Moreover, the regions of interest in an *n*-dimensional digital frequency domain for a discrete-time Volterra model or other equivalent discrete-time models (e.g. a NARX model) is the input frequency subdomains defined by

$$\varpi_i \leq \frac{\pi}{n} \quad or \quad f_i \leq \frac{1}{2n} \quad (normalised \quad frequency) \tag{4.8}$$

4.4 Visualisation Of GFRFs Defined In Higher Dimensions

Visualization is the use of graphical representations to make certain characteristics or values more apparent. Visualization conveys information by employing geometric forms, surfaces, solids and colours that are mapped to data values in particular ways.

In terms of the problems in this paper, the advantage of graphical methods to understand the concepts of input and output frequency subdomains has been shown in §4.1 and §4.2. Graphical techniques for the visualisation of a function with two variables are well established and applications to the analysis of the second order generalized frequency response functions are documented in numerous papers. However, although many nonlinear systems can be adequately described by a truncated Volterra series, which reduces the complexity of the problem, for a more accurate approximation, a Volterra model of at least third order is required in many cases. Therefore methods for exploring the properties of the third order GFRF need to be developed. This section introduces visualization techniques for both the magnitude and phase frequency response functions of a third order nonlinear system. Further analysis will be introduced in Part 2 of the paper using these graphical techniques

To illustrate the development, consider a cubic nonlinear system described by a polynomial NARX model with a simple input nonlinearity

$$y(k) = y(k-1) - 0.9y(k-2) + 0.5u(k-1) + 0.8u^2(k-1) + 0.2u^3(k-1) \tag{4.9}$$

The second order GFRF is computed using the recursive probing algorithm (Peyton Jones and Billings 1989), to give

$$H_2(j\omega_1, j\omega_2) = \frac{0.8 \quad e^{-j(\omega_1+\omega_2)}}{1 - e^{-j(\omega_1+\omega_2)} + 0.9e^{-2j(\omega_1+\omega_2)}} \tag{4.10}$$

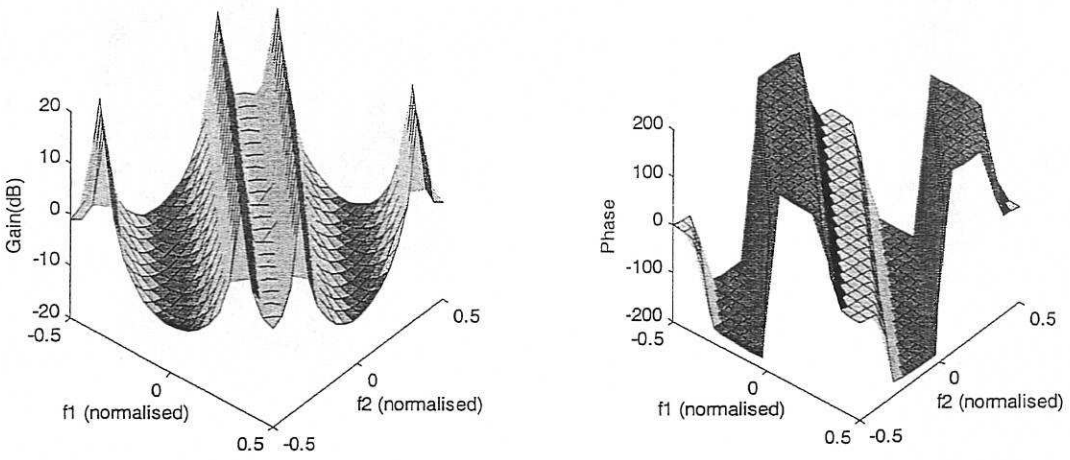

(a) The magnitude frequency response

(b) The phase frequency response

Fig. 7 The magnitude and phase plots of $H_2(j\omega_1, j\omega_2)$ in equation (4.10)

The magnitude and phase response of this system can be easily visualized using the plots in Fig. 7.

For the third order GFRF, which is given by

$$H_3(j\omega_1, j\omega_2, j\omega_3,) = \frac{0.2e^{-j(\omega_1+\omega_2+\omega_3)}}{1 - e^{-j(\omega_1+\omega_2+\omega_3)} + 0.9e^{-2j(\omega_1+\omega_2+\omega_3)}} \tag{4.11}$$

a graphical representation similar to Fig. 7 , but with one of three frequencies fixed, only reveals a partial image, from which only a limited amount of information about the third order GFRF can be gained. In this section, a set of "Volume Visualization" techniques will be introduced to give an overall view of the third order response function. Volume visualization is the creation of graphical representations of functions that are defined on three-dimensional

grids. To implement these techniques, H_3 is deliberately sampled at equal frequency intervals, typically at 0.05 normalized frequency. Fig. 8 shows a graph of the magnitude response function of H_3 given by one of these techniques, where each ball at a lattice point represents the magnitude of H_3 at that point and the magnitude value is indicated by the size of the ball. Such graphs are very helpful in observing the spatial distribution of H_3. Further information about the overall structure of H_3 can be gained by using another technique called "Isosurface". Isosurfaces are constructed by creating a surface within a three-dimensional frequency space that has the same value at each vertex. Isosurface plots are similar to contour plots in that they both indicate where values are equal. The application of isosurface techniques for this example is shown in Fig. 9, where the value of each isosurface is suggested by its colour.

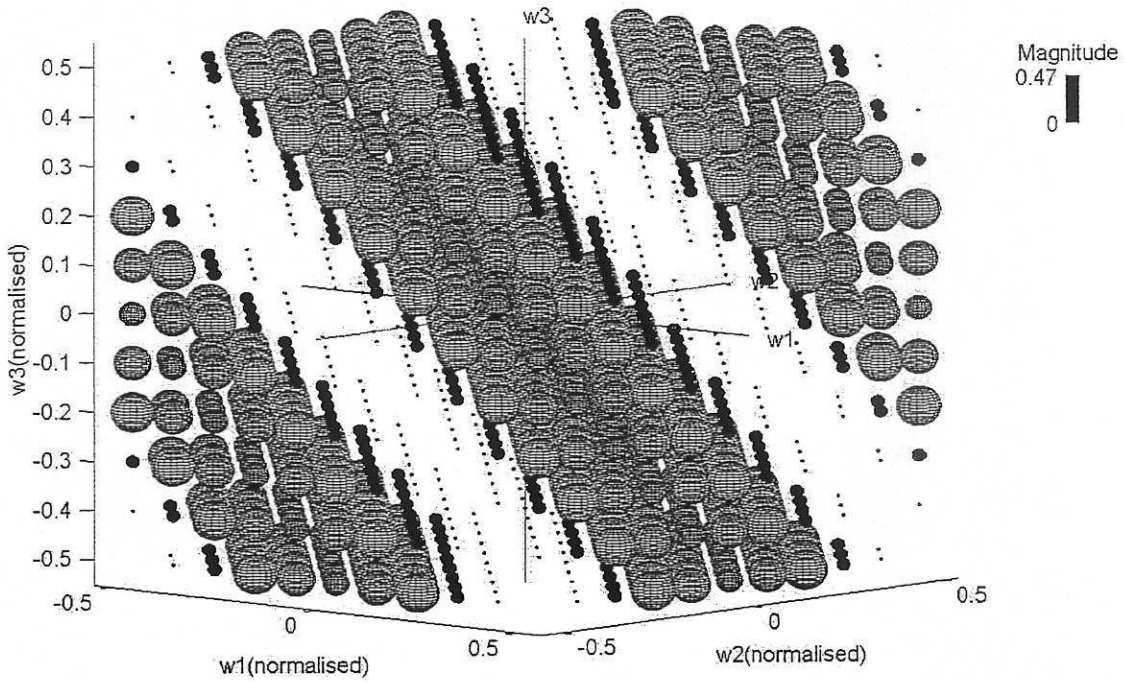

Fig. 8 The magnitude frequency response of H_3 given by equation (4.11)

Visualisation of the phase frequency response of H_3 is treated in a different way. The calculation of the phase response using the inverse tangent function constrains the results in the principal value range $[-\pi, \pi]$. This feature allows the phase response to be viewed as a vector with only two possible directions. Fig. 10 displays the phase response of H_3 using a "coneplot" technique which plots the phase response as cones pointing in either an upward or a downward direction, depending on whether the phase response at the corresponding point is positive or negative.

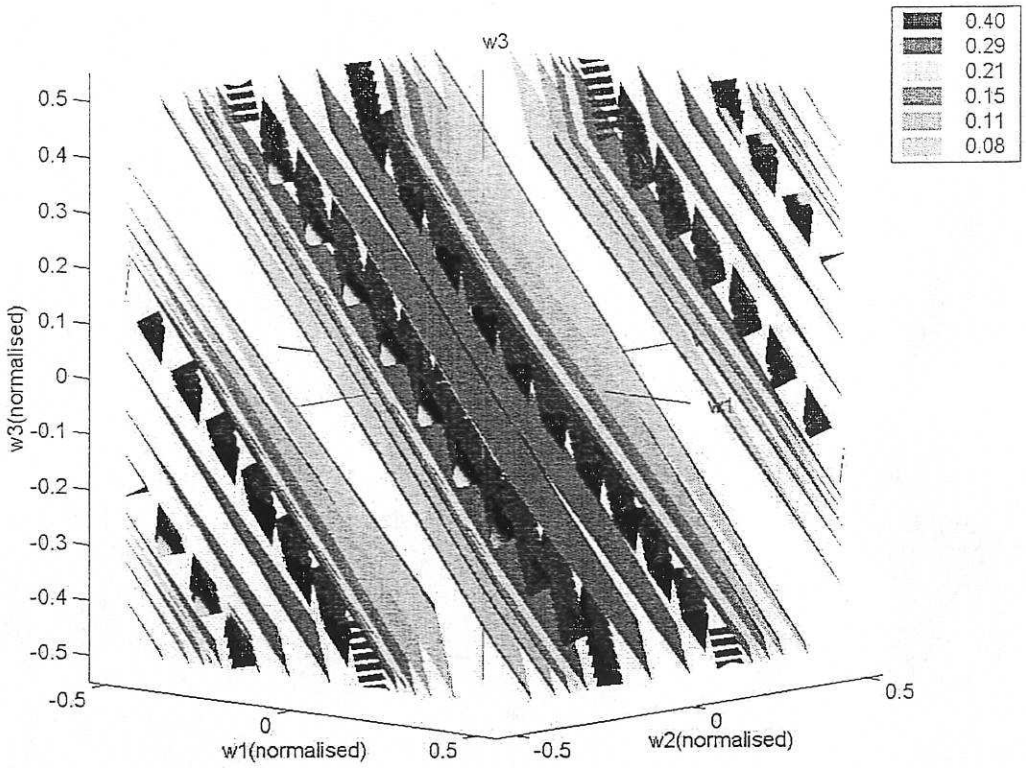

Fig. 9 The Isosurfaces of the magnitude frequency response of H_3 given by (4.11)

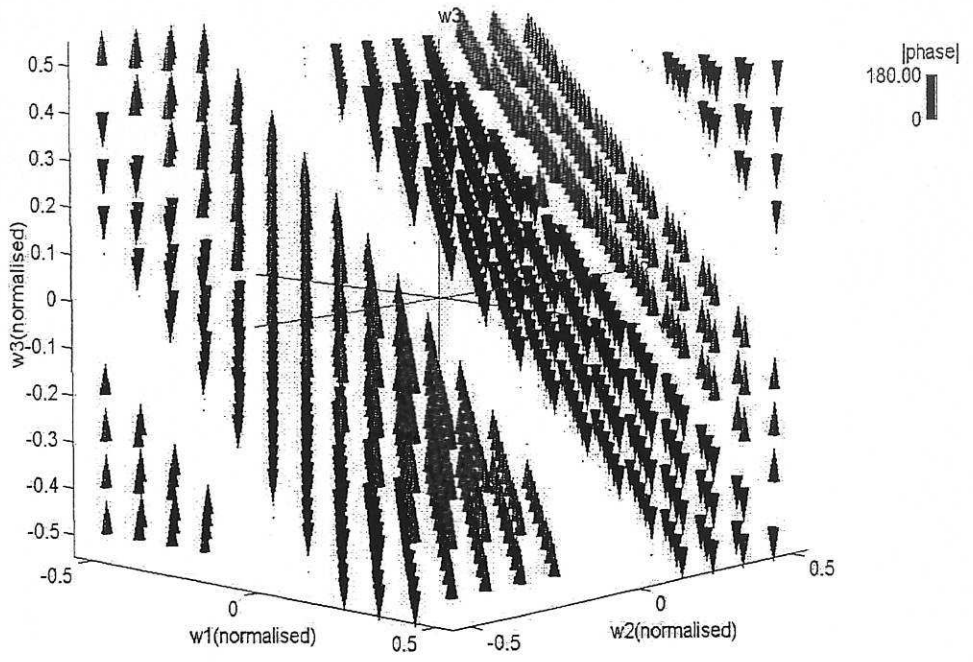

Fig. 10 The phase frequency response of H_3 given by equation (4.11)

5. Conclusions

The concept of input/output frequency subdomains has been presented to expose the relationship between one dimensional (where the input/output spectrum exists) and multidimensional (where generalised frequency response functions are defined) frequency spaces. The new graphical techniques have been introduced to allow the visualisation of the magnitude and phase of a third order GFRF for the first time.

Part 2 of this paper will present symbolic expansion techniques to reveal the structure of GFRFs. Based on these results, new methods are developed to analyse the characteristics of GFRFs graphically and symbolically.

Acknowledgements

S.A.B gratefully acknowledges that part of this work was supported by the UK Engineering and Physical Sciences Research Council and R.Y acknowledges the support provided by the University of Sheffield under the scholarship scheme.

References

Bedrosian, E., and Rice, S. O., 1971, The output properties of Volterra systems driven by harmonic and Gaussian inputs. *Proceedings of the Institute of Electrical and Electronics Engineers*, 59, 1688- 1707.

Bendat, J.S., 1990, Nonlinear system analysis and identification from random data. (Wiley, New York, 1990)

Billings, S. A., and Yusof, M. I., 1996, Decomposition of generalised frequency response functions for nonlinear systems using symbolic computation. *International Journal of Control*, 65, 589- 618.

Billings S.A., Zhang H., 1994, Analysing non-linear systems in the frequency domain part II: The phase response. *Mechanical Systems and Signal Processing*, 8(1), 45- 62.

Billings, S. A., and Peyton Jones, J. C., 1990, Mapping nonlinear integro-differential equation into the frequency domain. *International Journal of Control*, 52, 863- 879.

Billings S.A., Tsang K.M., 1989a, Spectral analysis for nonlinear systems Part I: Parametric nonlinear spectral analysis. *Mechanical Systems and Signal Processing*, 3, 319- 339; 1989 b, Spectral analysis for nonlinear systems Part II: Interpretation of nonlinear frequency response functions. *Mechanical Systems and Signal Processing*, 3, 341- 359.

Billings S.A, Korenberg M.J, Chen S., 1988, Identification of non-linear output-affine systems using an orthogonal least-squares algorithm. *Int.J.System Science*, 19 (8), 1559-1568, Aug

Boaghe O.M, Billings S.A., 2000, Dynamic wavelet and equivalent models. *European Journal of Control*, 6 (2), 120-131

Boyd S., Tang Y.S., and Chua L.O., 1983, Measuring Volterra Kernels. *IEEE Transactions on circuits and Systems,* Vol CAS-30, No.8, August, 571-577.

Brilliant M.B., 1958, Theory of the Analysis of Nonlinear Systems. Technical Report 345, MIT, Research Laboratory of Electronics, Cambridge, Mass, March 3.

Brillinger D.R., 1970, The identification of polynomial systems by means of high order spectra. Journal of Sound and Vibration, Vol 12, No 3, 301-331

Bussgang, J. J., Ehrman, L., and Garham, J. W., 1974, Analysis of nonlinear systems with multiple inputs. *Proceedings of the Institute of Electrical and Electronic Engineers*, 62, 1088 -1119.

Chua L.O and Ng C.Y., 1979, Frequency domain analysis of nonlinear systems: general theory. IEE Journal of Electronic Circuits and Systems. Vol 3, No.4, 165-185

Chua L.O and Liao, Y., 1989, Measuring Volterra Kernels (II). Int.J.Circuit Theory Appl., 17, 165-185, 1989

Collis W.B., White P.R. and Hammond J.K., 1998, Higher-order spectra: the bispectrum and trispectrum. *Mechanical Systems and Signal Processing,* 7(2), 173-189.

Fung C.F., Billings S.A., Luo W., 1996, On-line supervised adaptive training using radial basis function networks. NEURAL NETWORKS 9 (9) 1597-1617 Dec

George D.A., 1959, Continuous nonlinear systems. Technical Report 355, MIT Research Laboratory Of Electronics, Cambridge, Mass. July 24.

Lang Zi-Qiang, Billings S.A , 1996, Output frequency characteristics of non-linear systems. Int.J.Control, 64 (6), 1049-1067

Leontaritis I.J, Billings S.A., 1985, Input-output parametric models for nonlinear systems; Part I - Deterministic Nonlinear Systems; Part II - Stochastic Nonlinear Systems; Int.J.Control, 41, 303-359.

Kim, K. I., and Powers, E. J., 1988, A digital method of modelling quadratically nonlinear systems with a general random input. *IEEE Transactions on Acoustic, Speech and Signal Processing*, 36, 1758-1769.

Korenberg M.J, Billings S.A, Liu Y.P, Mcilroy P.J., 1988, Orthogonal parameter-estimation algorithm for non-linear stochastic-systems. Int.J.Control, 48 (1), 193-210 Jul

Nam S.W, Powers E.J., 1994, Application of higher-order spectral-analysis to cubically nonlinear-system identification. *IEEE Transactions on signal processing*, 42 (7): 1746-1765 JUL 1994

Narayanan S., 1970, Application of Volterra series to intermodulation distortion analysis of transistor feedback amplifiers. *IEEE Transactions on circuits and systems*, Vol 17, No.4, 518-527 Nov

Narayanan S., 1967, Transistor distortion analysis using Volterra series representation. Bell System Tec.J., Vol 46, No.5, 991-1024

Peyton Jones, J. C., and Billings, S. A., 1990, Interpretation of nonlinear frequency response functions. *International Journal of Control*, 52, 319-346.

Peyton Jones, J. C., and Billings, S. A., 1989, A recursive algorithm for computing the frequency response of a class of nonlinear difference equation models. *International Journal of Control*, 50, 1925-1949.

Rugh, W. J., 1981, *Nonlinear System Theory: the Volterra/Wiener Approach* (Baltimore, Maryland, U.S.A.: Johns Hopkins University Press).

Schetzen M., 1980, The Volterra and Wiener Theories of Nonlinear Systems. Chichester: John Wiley

Vinh T., Chouychai T., Liu H., and Djouder M., 1987, Second order transfer function: Computation and physical interpretation. *Proceedings of the Fifth International Model Analysis Conference*, London, U.K., pp. 587-592.

Weiner, D. D., and Spina, J. F., 1980, *Sinusoidal Analysis and Modelling of Weakly Nonlinear Circuits* (New York: Van Nostrand Reinhold).

Wiener N., 1958, Nonlinear Problems in Random Theory. MIT Press, Cambridge, Mass.

Worden K., Stansby P.K., Tomlinson G.R. and Billings S.A., 1994, Identification of non-linear wave forces. *Journal of Fluids and Structures,* 8, 19- 71.

Zhang H., Billings S.A. and Zhu Q.M., 1995, Frequency-response functions for nonlinear rational models. *International Journal of Control*, 61(5), 1073-1097.

Zhang H., Billings S.A., 1993, Analysing non-linear systems in the frequency domain part I: The transfer function. *Mechanical Systems and Signal Processing*, 7(6), 531- 550.